

Evidence for dielectric aging due to progressive 180° domain wall pinning in polydomain Pb(Zr_{0.45}Ti_{0.55})O₃ thin films

Pavel Mokry,^{1, a)} Yongli Wang,^{2, b)} Alexander K. Tagantsev,² Dragan Damjanovic,² Igor Stolichnov,² and Nava Setter²

¹⁾*Institute of Mechatronics and Computer Engineering, Technical University of Liberec, CZ-46117 Liberec, Czech Republic*

²⁾*Department of Materials, Ceramics Laboratory, EPFL Swiss Federal Institute of Technology, CH-1015 Lausanne, Switzerland*

(Dated: Received 2 October 2008; revised manuscript received 19 December 2008)

An evidence that the dielectric aging in the polydomain Pb(Zr_{0.45}Ti_{0.55})O₃ thin films is controlled by progressive pinning of 180° domain walls is presented. To provide such a conclusion, we use a general method, which is based on the study of the time evolution of the nonlinear, but anhysteretic, dielectric response of the ferroelectric to a weak electric field. A thermodynamic model of the ferroelectric system where the dielectric response is controlled by bending movements of pinned 180° domain walls is developed. Within this model, the nonlinear permittivity of the ferroelectric is expressed as a function of the microstructural parameters of the domain pattern. It is shown that by using the analysis of the time evolution of the nonlinear permittivity, it is possible to estimate changes in the concentration of the pinning centers that block the movements of the 180° domain walls during aging in polydomain perovskite ferroelectrics.

PACS numbers: 77.80.Dj

Keywords: Ferroelectric domain wall, Domain structure, Dielectric aging, Progressive pinning of domain walls, Nonlinear permittivity

I. INTRODUCTION

Aging of dielectric properties represents an unwanted feature in ferroelectric ceramics and lead zirconate-titanate (PZT) thin films, in particular, since it prevents their use in devices, which require very stable functional properties. It is believed that the origin of the dielectric aging in PZT and other similar perovskite ferroelectrics is caused by a rearrangement of pinning centers that block the movements of domain walls at more points and reduces the domain wall (extrinsic) contribution to permittivity of the ferroelectric.¹ In the following text, we will call this concept aging due to *progressive pinning*. Unfortunately, examples of credible evidence for the progressive pinning concept are still rather scarce^{1,2} due to strongly limited possibilities of experimental techniques. Even the direct observation of domain wall pinning itself is very rare and requires quite advanced experimental techniques^{3,4}. For this reason, progress in understanding the detailed role of domain wall pinning in phenomena such as fatigue, aging, or imprint⁵ is rather complicated, since it relies mainly on indirect measurements. One possibility to mention here is the study of the domain wall dynamics using measurements of the small-signal dielectric response,^{6–8} which is very sensitive to the pinning of the domain walls. Unfortunately, these experiments were analyzed using models, which cannot serve any quantitative

information on concentration of the pinning centers at the domain wall, etc.

The aforementioned issues have motivated the study presented below, where we will apply a general method introduced recently in Ref.⁹ that allows us to provide evidence that the dielectric aging of polydomain PZT films is controlled by progressive pinning of 180° domain walls. The adopted method is based on the measurement of the *nonlinear dielectric response* of non-polar polydomain ferroelectric samples to a *weak electric field*. This approach has several advantages. First, the application of a weak electric field to the ferroelectric sample has a minimum effect on the aging process. It is known that the electric cycling of the ferroelectric sample with electric fields comparable (in magnitude) to the coercive field has a strong deaging effect.¹⁰ Second, the dielectric response of the polydomain ferroelectric sample to the weak electric field is *anhysteretic*,¹¹ since it is controlled only by a fast reversible movement of the domain walls. This makes it possible to adopt a much simpler theoretical treatment in our analysis. It follows from the symmetry reasons that in the limit of the electric field tending zero, the permittivity ϵ_f of the polydomain non-polar ferroelectric sample (i.e., with the equal volumes of domains with the vectors of spontaneous polarization oriented along and against the applied electric field) is quadratically dependent on the electric field E ,

$$\epsilon_f(E) = \epsilon_L + bE^2, \quad (1)$$

where ϵ_L is the small-signal permittivity and b is the dielectric nonlinearity constant. This is in contrast to the essentially hysteretic dielectric response of the ferroelectric to the subswitching electric field, which is accom-

^{a)}Electronic mail: pavel.mokry@tul.cz

^{b)}Present address: Ceramic Components Division, EPCOS OHG, Siemensstrasse 43, 8530 Deutschlandsberg, Austria

panied by the Rayleigh-type linear electric field dependence of permittivity due to the irreversible movement of the domain walls.^{12–17} Nevertheless, one should note that there may arise experimental situations where even the practically small applied electric field breaks the limits for the irreversible movements of the domain walls and, therefore, violates the condition of the limit of the electric field tending zero. Thus, one should very carefully check that the experimental conditions satisfy the conditions for the applicability of the model.

The final advantage of the adopted method to study the nonlinear permittivity of the ferroelectric polydomain system in a weak electric field is that in this case, we do not need to strictly identify the microscopic origin of the domain wall pinning. The reason is that in weak electric fields the extrinsic contribution to the permittivity is controlled by fast reversible bending movements of the domain walls disregarding the nature of the pinning mechanism. Even if, in a particular sample, the domain wall pinning is strong due to many isolated crystal lattice impurities or it is weak due to the fluctuations of random fields in the vicinity of the domain wall, in a weak electric field, the pinning effect of both the random bonds or random fields results only in the bending of the domain wall. It means that our analysis can be reduced down to the problem of the identification of the bending movements of pinned domain walls. For that reason, the key elements of our analysis is the development of the model for the description of bending movements pinned 180° domain walls. Within this model, we consider that the progressive pinning changes the bending condition of the domain wall during aging, which affects both the small signal permittivity ε_L and the dielectric nonlinearity constant b .

We will show that if the dielectric aging is caused by progressive pinning and is controlled by bending movements of 180° domain walls, there exists the following relation between time dependencies of the small-signal permittivity $\varepsilon_L(t)$ and the dielectric nonlinearity constant $b(t)$:

$$\sqrt{b(t)} \propto \varepsilon_L(t) - \varepsilon_c, \quad (2)$$

where ε_c is the time-independent permittivity of the crystal lattice along the ferroelectric axis. To achieve the result announced above and given by Eqs. (1) and (2), we first present, in Sec. II, the details of our model of a ferroelectric film, where the movements of 180° domain walls are locally blocked by pinning centers. By applying a straightforward thermodynamic methodology presented in Sec. III, we calculate the linear and nonlinear parts of the extrinsic contribution to permittivity controlled by bending movements of the pinned 180° domain walls. In Sec. IV, we show that in the progressive pinning aging scenario there exists a characteristic relation between the linear and nonlinear domain wall contributions to permittivity of the polydomain ferroelectric. We demonstrate that by using measurements of the time evolution of the nonlinear permittivity it is possible to obtain evidence

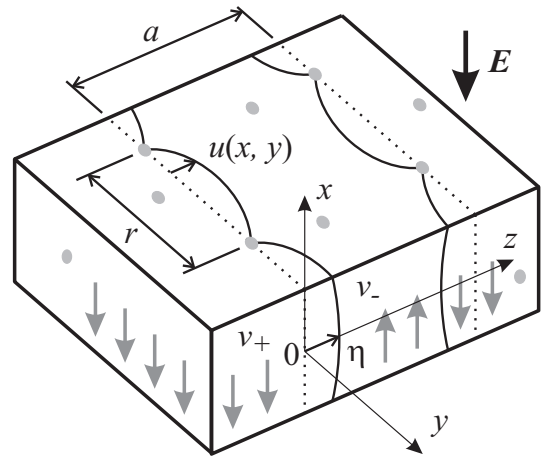


FIG. 1. Model of 180° domain wall bending. Planar position of the domain wall (dotted line) is locally blocked by pinning centers (gray circles). Orientation of the vector of spontaneous polarization is indicated by gray arrows. When the external electric field E is applied to the ferroelectric film, the domain wall is bent between pinning centers and the profile of the wall deflection is described by the function $u(x, y)$.

on whether the dielectric aging is controlled by the progressive pinning of 180° domain walls or not. Section V presents an application of our theory to aging experiments in [111]-oriented PZT (45/55) thin films.

II. MODEL OF 180° DOMAIN WALL BENDING

Figure 1 shows the model of a ferroelectric film with a lamellar 180° ferroelectric domain pattern, where the average distance between the domain walls (domain wall spacing) is denoted by the symbol a . We consider that the top and bottom electrodes of the film are perpendicular to the ferroelectric axis x of the attached Cartesian coordinate system. Using the “hard ferroelectric” approximation, we express the electric displacement within each ferroelectric domain as a sum of the spontaneous polarization P_0 (whose orientation differs from domain to domain) and the linear dielectric response of the crystal lattice to the electric field,

$$D_x = \varepsilon_0 \varepsilon_c E_x \pm P_0, \quad (3a)$$

$$D_{y,z} = \varepsilon_0 \varepsilon_a E_{y,z}, \quad (3b)$$

where ε_c and ε_a are the components of the permittivity tensor of the crystal lattice in the directions along and perpendicularly to the ferroelectric axis, respectively, and ε_0 is the permittivity of vacuum.

In the absence of the electric field, we consider the domain pattern to be neutral, i.e., that the volume fractions v_+ and v_- of the adjacent antiparallel domains are the same, and that the 180° domain walls are parallel to the x - y plane and pinned by immobile pinning centers, which are distributed in the x and y directions with an average

distance r between them. Thus, the pinning center density on the domain wall is proportional to $1/r^2$.

When the electric field E is applied to the ferroelectric film, it exerts a pressure $-2P_0E$ on the domain wall and it bends the originally planar domain wall between the pinning centers. The domain wall bending produces a change in the volume fractions v_+ and v_- of the domains with the spontaneous polarization oriented along and against the applied electric field, respectively. On the other hand, the domain wall deflection produces an increase in the domain wall area. Since the bent domain wall is no longer parallel to the vector of spontaneous polarization, a bound charge $\sigma_b = -\Delta P_{0,n}$ appears on the domain wall due to the discontinuous change in the normal component of spontaneous polarization at the domain wall. If we denote the domain wall displacement in the z direction by the function $u(x, y)$, its exact profile is given by minimizing the thermodynamic potential G_w , which consists of the depolarizing field energy, the energy associated with the crystal lattice polarization, the energy of the domain wall, and the energy supplied to the system by the external electric source. In this model, it yields the solution of Euler-Lagrange equation, which was analyzed earlier.³

In order to calculate the extrinsic contribution to the permittivity due to bending movements of pinned domain walls, we approximate the generally random distribution of pinning centers by a periodic one with equidistant pinning centers, but with the same average density $1/r^2$. We consider that the pinning centers divide the infinite area of the domain wall into square segments with edges parallel to the x and y directions in such a way that each segment of the domain wall is pinned at its corners and the domain wall can move freely in the interior of each segment, as indicated in Fig. 1. This approximation reflects the assumption that the main contribution to the permittivity is coming from the structures on the domain wall with the periods that are close to the mean period in the system r . The strict procedure would be to expand the random distribution of the pinning centers in the Fourier series. Our approximation is good if the Fourier spectrum is not very wide. The consideration of the periodicity of pinning centers in the direction of the film thickness also limits the applicability of the domain wall bending model to samples of thicknesses much greater than the average pinning centers distance, i.e., $h \gg r$.

Finally, in most ferroelectric materials as well as in the samples used in our experiments, it is easy to show that even small domain wall displacements (about a lattice constant) are sufficient to produce the observed values of extrinsic contributions to the permittivity. Therefore, it is fully justified to consider that the maximum deflection η of the domain wall is much smaller than the average distance between pinning centers r . In this case, if we take the origin of the coordinate system in the middle of each square segment, it is convenient to approximate the profile of the domain wall deflection in this segment by a

parabolic function of the form,

$$u(x, y) = \eta \left[1 - 4 \frac{\alpha x^2 + y^2}{r^2(1 + \alpha)} \right], \quad (4)$$

where η is the maximum deflection of the domain wall and the parameter α is introduced in order to take into account the anisotropy of the radius of curvature of the bent domain wall due to the strong depolarizing effect in the direction of the ferroelectric x axis. Coordinate values of x and y are running over the interval from $-r/2$ to $r/2$.

III. EXTRINSIC PERMITTIVITY

When the alternating electric field is applied to the ferroelectric sample, the domain walls start to vibrate between the pinning centers, which results in a change in the volume fractions v_+ and v_- of the antiparallel domains, where $v_+ + v_- = 1$. This represents the source of the extrinsic contribution to the permittivity of the ferroelectric film. To calculate the extrinsic contribution to the permittivity, it is convenient to consider the net spontaneous polarization P_N , which is given by the difference in the volume fraction of domains with the vector of spontaneous polarization oriented along and against the applied electric field, i.e., $P_N = (v_+ - v_-) P_0$, and which can be expressed in the form,

$$P_N = \frac{2P_0}{ar^2} \int_A u(x, y) dA = \frac{4\eta}{3a} P_0. \quad (5)$$

where the integral is taken over the square segment A , while x and y are running from $-r/2$ to $r/2$. In the following text, we will use the above expression to measure the maximum deflection of the domain wall in terms of the net spontaneous polarization, i.e., $\eta = (3a P_N)/(4 P_0)$. The response of the net spontaneous polarization with respect to the applied electric field E is controlled by the thermodynamic function G_w per unit volume of the ferroelectric,

$$G_w = \Phi_s(P_N) + \Phi_{\text{dep}}(P_N) - P_N E, \quad (6)$$

where the functions

$$\Phi_s = \frac{1}{ar^2} \int_A \sigma_w \sqrt{1 + u_x^2(x, y) + u_y^2(x, y)} dA \quad (7)$$

and

$$\Phi_{\text{dep}} = \frac{1}{ar^2} \int_A \frac{1}{2} \sigma_b \varphi_d \sqrt{1 + u_x^2(x, y) + u_y^2(x, y)} dA \quad (8)$$

represent two contributions to the thermodynamic function G_w due to the increase in the domain wall area and due to the depolarizing field, respectively. In Eqs. (7) and (8), the integrals are taken over the square segment A where x and y are running from $-r/2$ to $r/2$, the symbol σ_w stands for the surface energy density associated

with the surface tension of the bent domain wall, and the symbol φ_d stands for the electrostatic potential on the domain wall associated with the depolarizing field, which is produced by the bound charges σ_b .

The function Φ_s can be calculated in a straightforward way by direct substitution of Eq. (4) into Eq. (7). The leading terms of Φ_s with respect to the net spontaneous polarization equal

$$\Phi_s \approx \frac{3a\sigma_w(1+\alpha^2)}{4r^2 P_0^2 (1+\alpha)^2} P_N^2 - \frac{9a^3\sigma_w(9+10\alpha^2+9\alpha^4)}{80 P_0^4 r^4 (1+\alpha)^4} P_N^4. \quad (9)$$

In order to express the function Φ_{dep} , it is necessary to calculate the spatial distribution of the electrostatic potential φ_d in the vicinity of the bent domain wall. Since this goes beyond the main scope of this paper, the detailed calculations of the functions φ_d and Φ_{dep} are presented in the Appendix A. Here we present only the result for the leading terms of the function Φ_{dep} with respect to the net spontaneous polarization,

$$\Phi_{\text{dep}} \approx \frac{0.174a\alpha^2}{\varepsilon_0 r (1+\alpha)^2 \sqrt{\varepsilon_a \varepsilon_c}} \left[P_N^2 - \frac{3a^2(1+1.43\alpha^2)}{2P_0^2 r^2 (1+\alpha)^2} P_N^4 \right]. \quad (10)$$

Now, the thermodynamic potential G_w per unit volume of ferroelectric can be expressed in the form of a Taylor expansion with respect to P_N . Disregarding the constant term, this function reads as

$$G_w \approx \frac{3aP_N^2}{4r^2(1+\alpha)^2} \left[\sigma_w \frac{(\alpha^2+1)}{P_0^2} + \frac{7.2r\alpha^2}{\pi^3 \varepsilon_0 \sqrt{\varepsilon_a \varepsilon_c}} \right] - \frac{9a^3 P_N^4}{80P_0^2 r^4 (1+\alpha)^4} \left[\sigma_w \frac{(9+10\alpha^2+9\alpha^4)}{P_0^2} + \frac{r\alpha^2(2.33+3.32\alpha^2)}{\varepsilon_0 \sqrt{\varepsilon_a \varepsilon_c}} \right] - P_N E, \quad (11)$$

where the first term in each square bracket is due to the increase in the energy of the surface tension of the bent domain wall and the second term is due to the increase in the depolarizing field energy produced by the bound charges at the domain wall.

In what follows, it will be convenient to express the surface energy density of the domain wall σ_w in the form,

$$\sigma_w \approx \frac{a_w P_0^2}{6\varepsilon_0 \varepsilon_c}, \quad (12)$$

where the parameter a_w is of the order of the domain wall thickness. The unknown value of the parameter α is determined from the condition

$$\partial G_w(P_N, E; \alpha) / \partial \alpha = 0. \quad (13)$$

Later, it will be checked that in the case of a stable domain pattern and for weak applied fields, the function

G_w is dominated by the lowest (quadratic) term. Under this consideration, we can find the minimum of the function G_w with respect to α and the condition given by Eq. (13) yields

$$\alpha_{\min} = \left(1 + \frac{1.4r}{a_w} \sqrt{\frac{\varepsilon_c}{\varepsilon_a}} \right)^{-1}. \quad (14)$$

In most of the samples, it is reasonable to consider that the domain wall thickness a_w is much smaller than the average distance between the pinning centers r , i.e., $a_w \ll r$, and, in this case, Eq. (14) can be further simplified as

$$\alpha_{\min} \approx \frac{a_w}{1.4r} \sqrt{\frac{\varepsilon_a}{\varepsilon_c}}. \quad (15)$$

After substitution of Eqs. (12) and (15) into Eq. (11), we obtain the following form for the expansion of the function G_w with respect to the net spontaneous polarization:

$$G_w(P_N, E) \approx \frac{a a_w}{8\varepsilon_0 \varepsilon_c r^2} P_N^2 - \frac{0.17 a^3 a_w}{\varepsilon_0 \varepsilon_c r^4 P_0^2} P_N^4 - P_N E. \quad (16)$$

It should be noted that in the case of most of the high-quality samples, $\alpha_{\min} \ll 1$ and the thermodynamic potential G_w is dominated by the surface tension, which can be readily seen after substituting Eqs. (12) and (15) into Eqs. (9) and (10).

The response of the net spontaneous polarization P_N to the applied electric field E can be found from the condition for the minimum of the function G_w ,

$$\partial G_w(P_N, E) / \partial P_N = 0 \quad (17)$$

and it can be expressed as a Taylor expansion with respect to the applied electric field,

$$P_N(E) \approx \frac{4\varepsilon_0 \varepsilon_c r^2}{a a_w} E + \frac{172.8 r^4 \varepsilon_0^3 \varepsilon_c^3}{a a_w^3 P_0^2} E^3. \quad (18)$$

Now we use the fact that the average electric displacement of the polydomain film along the ferroelectric axis D_f is given by the sum of the linear dielectric response of the crystal lattice to the electric field and the net spontaneous polarization, i.e., $D_f(E) = \varepsilon_0 \varepsilon_c E + P_N(E)$. Later we will check that the dielectric nonlinearity of the whole system is dominated by the bending mechanism and, in this case, the field dependence of permittivity of the ferroelectric polydomain film can be expressed in the form

$$\varepsilon_f(E) \approx \varepsilon_c + \varepsilon_w + bE^2, \quad (19)$$

where ε_c is the intrinsic permittivity along the spontaneous polarization and

$$\varepsilon_w(r, a) \approx \frac{4\varepsilon_c r^2}{a a_w}, \quad (20)$$

$$b(r, a) \approx \left(\frac{1}{4} \right) \frac{518.4 r^4 \varepsilon_0^2 \varepsilon_c^3}{a a_w^3 P_0^2} \quad (21)$$

are the coefficients of the small-signal linear and the quadratic terms of the extrinsic contribution to permittivity with respect to the applied electric field, respectively. Here it should be noted that Eq. (18), is actually derived for the case of the dc field dependence of the net spontaneous polarization on the applied electric field. On the other hand, the experimental part of the paper addresses the ac field amplitude dependence of the average (mean) permittivity. Therefore, the relations given by Eqs. (20)-(21) are expressed for the ac field amplitude dependence of the average (mean) permittivity and the coefficient b differs from the corresponding term in Eq. (18) by a factor $1/4$.

IV. PROGRESSIVE PINNING OF DOMAIN WALLS AND DIELECTRIC AGING

Now it is seen that values of the small-signal extrinsic permittivity ε_w and of the dielectric nonlinearity coefficient b are controlled by the domain pattern configuration, i.e., by the pinning center average distance r and by the domain spacing a . It is natural to expect that the parameters r and a can evolve with time, which may represent a source of aging of the dielectric response and, therefore, a source of the time evolution of the field dependence of permittivity $\varepsilon_f(E)$. However, one should first identify the thermodynamic force, which can drive the system to evolve with time and which can be responsible for the aging process.

First let us focus on the possible role of the domain spacing a in the process of aging. In real systems, the domain pattern is usually controlled by the prehistory of the sample so that the domain spacing may be essentially different from its equilibrium value at the given temperature. It means that there clearly exists a thermodynamic force that drives the system to reach the state with the equilibrium domain spacing. This thermodynamic force actually originates from the competition between the energy of the domain walls, the electrostatic energy, and the surface energy at the interface between the ferroelectric and the electrode.¹⁸⁻²¹ Nevertheless, frequent observations of rather stable but essentially nonequilibrium domain patterns^{22,23} represent a clear indication that these energies are usually much weaker than the energies involved in the pinning-depinning processes during the domain wall movement under the application of sub-switching electric fields. Therefore, it is not very reasonable to consider that the possible change in the domain spacing could be responsible for the aging of the dielectric response.

The second scenario, which can be described within our domain wall bending model, is the *progressive pinning of the domain walls*. Although it has been already mentioned in Sec. I that one can apply the domain wall bending model on the weak-field nonlinear permittivity data disregarding the origin of pinning, one particular mechanism in perovskite ferroelectrics to mention here

is pinning by the orientation of dipole defects.¹ This model is based on the interaction of the domain walls with the dipoles formed by an acceptor ion (e.g., Ni²⁺, Fe²⁺, etc.) at the Ti⁴⁺ site and an oxygen vacancy in the surrounding oxygen octahedron. Since the free energy of the dipole defect in ferroelectrics depends on its orientation with respect to the vector of spontaneous polarization, the thermodynamic force—which drives the dipole defects to align with the spontaneous polarization vector in each domain in order to minimize the free energy of the whole system—causes an increase in the number of pinning centers that blocks the domain wall movement under a weak electric field. Thus, the increase in the number of such pinning centers naturally results in the decrease in the average distance r between them.

Our model for bending movements of 180° domain walls makes it possible to identify such aging process using measurements of nonlinear permittivity. We can express the average distance between pinning centers r from Eq. (20) and substitute it into the formula for the dielectric nonlinearity coefficient b given by Eq. (21). This gives the relation between the parameters b and ε_w in the form,

$$b \approx \frac{8.1 \varepsilon_0^2 \varepsilon_c}{P_0^2} \left(\frac{a}{a_w} \right) \varepsilon_w^2. \quad (22)$$

If such a relation between ε_w and b , which is typical for this aging process and which is quite different from the prediction of, e.g., the Landau theory, is identified in the aging measurements, it gives a reasonable hint that the progressive pinning mechanism is responsible for the dielectric aging of polydomain ferroelectrics. Therefore, the principal result of this work is that by considering the domain wall bending mechanism and using the analysis of the time evolution of the nonlinear dielectric response, we can provide evidence that the dielectric aging is controlled by the progressive pinning of the 180° domain walls.

In addition, we can study the evolution of the pinning centers concentration at the domain walls. By combining Eqs. (20) and (21) and by eliminating the average domain spacing, one can estimate the time dependence of the average pinning center distance according to the following formula:

$$r(t) = \frac{0.175 a_w P_0}{\varepsilon_0 \varepsilon_c} \sqrt{\frac{b(t)}{\varepsilon_w(t)}}. \quad (23)$$

V. EXPERIMENTAL VERIFICATION

In this section, we present a direct way of the experimental verification of the considered model for bending movements of the pinned domain walls to PZT ferroelectric films of tetragonal symmetry. Our model can be directly applicable to [001]-oriented PZT films. Unfortunately, there exists a reason, which makes the use of

[001]-oriented PZT films not very practical to demonstrate the relevance of the domain wall bending model. Namely, the domain composition of c and/or a domains is difficult to control in such films. Because of the large dielectric anisotropy of PZT, this makes it difficult to control the lattice contribution to the permittivity. On the other hand, it appears to be convenient to use [111]-oriented films; since their lattice contribution is unique and independent on the domain pattern configuration, all 180° domain walls have the same orientation with respect to the applied electric field and, thus, they contribute identically to the dielectric response. These features are important in applying our model to experimental data. Since the application of our model to [111]-oriented PZT films requires some modifications, we describe the application of the domain wall bending model to the both particular cases separately.

A. Application to [001]-oriented PZT films

To prove that the progressive aging scenario is responsible for the evolution of the dielectric response, we need to distinguish the extrinsic $\varepsilon_w + bE^2$ from the intrinsic ε_c contributions to the field dependence of the permittivity $\varepsilon_f(E)$. Since it is natural to expect that the intrinsic contribution to the permittivity ε_c does not change in time, we can compare the measured small-signal permittivity ε_L , given by the formula,

$$\varepsilon_L = \varepsilon_f(0) = \varepsilon_c + \varepsilon_w, \quad (24)$$

with the dielectric nonlinearity constant b , which can be determined from the experimental data using the following expression:

$$b = [\varepsilon_f(E) - \varepsilon_L] / E^2. \quad (25)$$

Then, with the use of Eq. (24), the relationship given in Eq. (22) can be rewritten in the form,

$$b \approx \frac{8.1 \varepsilon_0^2 \varepsilon_c}{P_0^2} \left(\frac{a}{a_w} \right) (\varepsilon_L - \varepsilon_c)^2. \quad (26)$$

Finally, taking the square root of b from the above equation, we arrive at the following relationship between ε_L and b , which can be cross checked experimentally:

$$\sqrt{b} \approx K \varepsilon_L - B, \quad (27)$$

where

$$K = \sqrt{\frac{8.1 \varepsilon_0^2 \varepsilon_c}{P_0^2} \left(\frac{a}{a_w} \right)}, \quad B = K \varepsilon_c. \quad (28)$$

Therefore the validity of Eq. (22) can be demonstrated by a linear relationship between the values of \sqrt{b} and the small-signal dielectric permittivity ε_L .

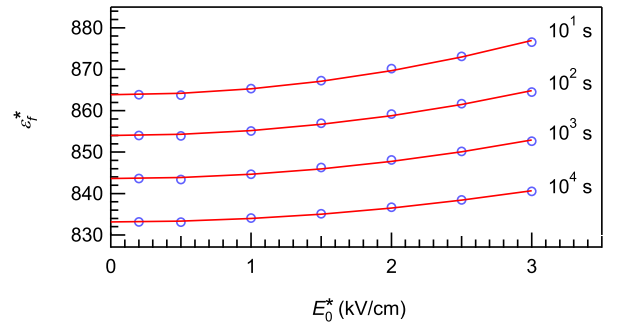


FIG. 2. (Color online) ac-field dependence of the dielectric permittivity (real part) within four decades of time. The measuring frequency was 1 kHz. The scattered markers represent the experimentally measured data. The solid lines are quadratic fittings using Eq. (19).

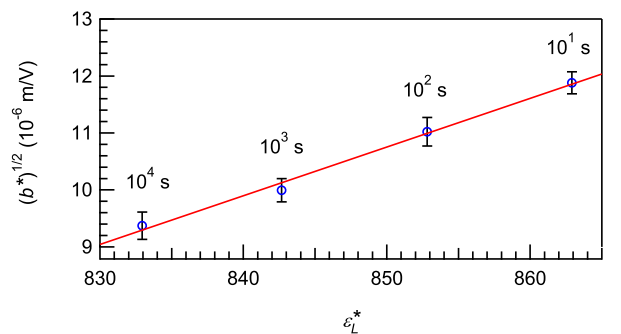


FIG. 3. (Color online) Linear dependence of the square root of the coefficient b^* of the quadratic term in the expansion of the permittivity with respect to the applied electric field on the total weak-field permittivity of the ferroelectric film.

B. Application to [111]-oriented PZT films

In the case of the [111]-oriented PZT films, one cannot apply our model in a such a straightforward way as it was done in Sec. V A. There are two main reasons for that. First, the bending movements of pinned 180° domain walls contribute to the value of the permittivity in the direction of the vector of spontaneous polarization. Second, perovskite ferroelectrics are materials with a rather large dielectric anisotropy in the directions parallel ε_c and perpendicular ε_a to the orientation of the vector of spontaneous polarization. In order to obtain reasonable numerical estimation of the microstructural parameters of the domain pattern, one should take the aforementioned point into account while interpreting the dielectric nonlinearity measurements. In the following text, we will denote all physical quantities, which are measured on the [111] oriented film, by a star superscript “*.”

The electric field dependence of the out-of-plane permittivity of the [111]-oriented PZT film in the tetragonal

phase $\varepsilon_f^*(E)$ is given by the formula,

$$\begin{aligned}\varepsilon_f^*(E) &= \varepsilon_f(E) \cos^2(\theta) + \varepsilon_a \sin^2(\theta) \\ &= (\varepsilon_c + \varepsilon_w + bE^2) \cos^2(\theta) + \varepsilon_a \sin^2(\theta),\end{aligned}\quad (29)$$

where E is the electric field along the vector of spontaneous polarization, the symbol θ stands for the angle between the spontaneous polarization and the normal to the plane of the film vector, which is equal to $\theta = \arctan(\sqrt{2}) = 54.7^\circ$. The value of E is given by the applied electric field in the [111] direction E^* , i.e., $E = E^* \cos\theta$. If we introduce the dielectric anisotropy factor ξ by the formula

$$\xi = \varepsilon_a/\varepsilon_c, \quad (30)$$

the measured small-signal permittivity ε_L^* and the dielectric nonlinearity constant b^* are then equal to

$$\varepsilon_L^* = \varepsilon_w \cos^2(\theta) + \varepsilon_c \left[\cos^2(\theta) + \xi \sin^2(\theta) \right], \quad (31)$$

$$b^* = b \cos^4(\theta). \quad (32)$$

Now we can follow the same procedure as in Sec. V A, i.e., we express the value of ε_w from Eq. (31) and we combine it with Eqs. (22) and (32). Finally, we obtain again the linear relationship between $\sqrt{b^*}$ and ε_L^* ,

$$\sqrt{b^*} \approx K^* \varepsilon_L^* - B^*, \quad (33)$$

where

$$K^* = K, \quad (34a)$$

$$B^* = \varepsilon_c K \frac{\xi + 1 - (\xi - 1) \cos(2\theta)}{2}, \quad (34b)$$

$$K = \sqrt{\frac{8.1 \varepsilon_0^2 \varepsilon_c}{P_0^2} \left(\frac{a}{a_w} \right)}. \quad (34c)$$

VI. RESULTS AND A DISCUSSION

The presented model of 180° domain wall bending was applied to study the evolution of the dielectric response in a [111]-oriented $\text{Pb}(\text{Zr}_{0.45}\text{Ti}_{0.55})\text{O}_3$ thin film (240 nm in thickness). The film was deposited via a standard sol-gel method on a Pt-coated Si substrate.¹³ Desired platinum patterns were vaporized on the surface of the crystallized film to form the top electrode. The out-of-plane dielectric response was measured using a Hewlett-Packard (HP) 4284A high-precision impedance analyzer. The film was first depoled with a fast-decayed low-frequency (1 Hz) ac field (the amplitude decays from 80 kV/cm to zero in five periods). The dielectric response was then recorded as a function of the ac driving field ($E_0 \leq 3$ kV/cm) and of the aging time at room temperature. The coercive field of the film is 60 kV/cm and, therefore, it is much larger than the maximum field used in this study.

Figure 2 shows the ac-field dependence of the dielectric permittivity within four decades of time, which can

be well fitted by the quadratic relation given in Eq. (19). This is in contrast to the Rayleigh-type relation, where the dielectric permittivity increases linearly with the ac field as a result of the irreversible movement of domain walls under subswitching fields (usually a few tens of kV/cm).^{12–17} The bending of 180° domain walls is actually a fast reversible process. Figure 3 shows the linear relationship between the values of $\sqrt{b^*}$ and the small-signal dielectric permittivity ε_L^* . Therefore, our experimental data unambiguously prove the validity of Eq. (33).

Using the fit of results presented in Fig. 3, we can estimate the lattice permittivity ε_c and the ratio a/a_w . This is done in two steps. First, the slope $K^* = 85 \times 10^{-9} \text{ mV}^{-1}$ and the offset $B^* = 62 \times 10^{-6} \text{ mV}^{-1}$ of the linear dependence of $\sqrt{b^*}$ versus ε_L^* are determined using a standard linear regression analysis. Second, the system of Eqs. (34) is solved by taking the values of spontaneous polarization $P_0 = 0.54 \text{ C/m}^2$ (Ref.²⁴) and the dielectric anisotropy factor $\xi = 3.3$.²⁵ Solution of the system of Eqs. (34) gives a value for the lattice permittivity ε_c equal to 280, which is in excellent agreement with the thermodynamic values,^{24,25} and for the ratio a/a_w equal to 12×10^3 . From Eq. (31), the small-signal extrinsic contribution to the permittivity along the spontaneous polarization ε_w is estimated to be decreasing from 388 down to 296 during the time of 10^4 s of the aging experiment. The bending mechanism contributes to the total weak-field permittivity along the spontaneous polarization by about 50%, which is also in agreement with the recent dielectric measurements of the weak-field permittivity of PZT ceramics in a very wide frequency range.²⁶ From the ratio $a/a_w = 12 \times 10^3$, we can estimate the average domain spacing using the domain wall thickness as found from the Landau-Ginzburg-Devonshire theory (0.7 nm) (Ref.²⁷) or by an ab-initio calculation (0.5 nm).²⁸ The average distance between adjacent 180° domain walls thus has a value of about $5.9 \mu\text{m}$. This specific distance is much larger than the typical grain size (~ 100 nm), indicating a low density of 180° domain walls. This is reasonable in the case of strongly clamped films, as was shown by the transmission electron microscopy (TEM) observation in Ref.¹⁴ In addition, the average distance between adjacent 180° domain walls is controlled by the prehistory of the sample and by the depoling process used before the aging experiment. Finally, our experiments indicate that the average distance between the pinning centers has decreased from 33 down to 29 nm during 10^4 s. These values, which are much smaller than the film thickness, correspond to the volume concentration of crystal lattice impurities being higher than 0.03%, which is acceptable since it is known that the nominally pure PZT ceramic films possess naturally occurring acceptor impurities.

Considering the key element of our method—the model of bending movements of pinned 180° domain walls—we have calculated the linear and nonlinear contributions to extrinsic permittivity in the polydomain ferroelectric and used this result to analyze our experimental data. As a

result, we were able to extract some microstructural parameters of the domain pattern, i.e., the average distance between the pinning centers and the domain spacing, and material parameters of the ferroelectric, i.e., the intrinsic permittivity of the crystal lattice. However, three important assumptions have been made during the development of the theoretical model and now it should be checked whether the values of the parameters fitted from our experimental data do not violate such assumptions: (a) the nonlinearity is dominated by bending of the 180° domain walls, (b) the maximum deflection of the bent domain wall is much smaller than the average distance between the pinning centers, and (c) the free energy G_w that controls the net spontaneous polarization response to the electric field $P_N(E)$ is dominated by the lowest (quadratic) term.

The first assumption can be verified by comparing the dielectric nonlinearity constant that is controlled by bending movements of the 180° domain walls b with the dielectric nonlinearity of the crystal lattice b_c , which is equal to⁹

$$b_c = \frac{12 \varepsilon_0^2 \varepsilon_c^3}{P_0^2} \left(1 - \frac{3\varepsilon_w}{8\varepsilon_c} \right).$$

By substituting the numerical results of our study, one can immediately see that $b_c = 1.6 \times 10^{-16} \text{ m}^2 \text{ V}^{-2}$, which is about 6 orders of magnitude smaller than the values observed in the experimental part of this study, i.e., $b \approx 8 \times 10^{-10} \text{ m}^2 \text{ V}^{-2}$.

The second assumption can be verified by using Eqs. (5) and (18). After the substitution of the numerical parameters fitted from our experiments, we can obtain that, at the maximum fields applied to our sample, i.e., 3 kV/cm, the maximum deflection η of the domain wall is about 17 nm. This value is more than two times smaller than the estimated average distance between the pinning centers r (over 40 nm).

The third assumption can be verified by the substitution of Eq. (5) into Eq. (11). With use of the numerical parameters fitted from our experiments, we can see that, at the maximum fields applied to our sample, i.e., 3 kV/cm, the value of the lowest (quadratic) term in the expansion of the thermodynamic function G_w is about 302 J m^{-3} . This value is more than three times greater than the value of the higher- (fourth-) order term, which is approximately -90 J m^{-3} .

Therefore, it is seen that all assumptions made in the theoretical part of our study are fully justified and applicable to real ferroelectric samples. By applying the main results of the theoretical model [Eqs. (19) to (22)] to our experimental data, we have provided a strong evidence that the dielectric nonlinearity in polydomain ferroelectrics is predominantly controlled by the considered bending mechanism. In addition, we have shown that from the evolution of the relation between the small-signal permittivity ε_L and the dielectric nonlinearity constant b it is possible to distinguish the microstructural mechanisms, which are responsible for the aging of the

dielectric response. In our particular experimental case, the linear relationship between the values of \sqrt{b}^* and ε_L^* provided us with evidence that the decrease in the linear dielectric permittivity during aging can be attributed to the increase in the average pinning center density on the domain wall, indicating a progressive pinning nature of the aging phenomenon. Finally, Eqs. (20) and (21) show that—from known values of the parameters ε_L and b at a given time—it is possible to estimate the actual values of the domain spacing a and the average pinning center density on the domain wall $1/r^2$. Therefore, we believe that our results can be used as a simple and useful tool for getting a deeper insight into the configuration of the domain pattern and the quality of ferroelectric thin films and for providing a way to identify the evolution of the 180° domain pattern microstructure in perovskite ferroelectrics.

ACKNOWLEDGMENTS

This work has been supported by the Czech Science Foundation under Project No. GACR 202/06/0411 and No. GACR 202/07/1289, by the Swiss National Science Foundation, and by the MIND - European network on Piezoelectrics. Authors thank Guido Gerra for reading the manuscript.

Appendix A: Electrostatic energy of the bent 180° domain wall

In this appendix, we present the detailed calculation of the electrostatic potential φ_d and the depolarizing field energy per unit volume of the ferroelectric Φ_{dep} with the bent 180° domain walls. When the domain wall is bent, the discontinuous change in the normal component of spontaneous polarization $P_{0,n}$ at the domain wall yields the appearance of a bound charge of surface density $\sigma_b = -\Delta P_{0,n}$,

$$\sigma_b(x, y) = \frac{-2P_0 u_x(x, y)}{\sqrt{1 + u_x^2(x, y) + u_y^2(x, y)}}, \quad (\text{A1})$$

where the functions $u_x(x, y)$ and $u_y(x, y)$ are the partial derivatives of the function $u(x, y)$ with respect to x and y , respectively. If the maximum deflection η of the domain wall is much smaller than the average distance between pinning centers r then by using Eq. (4), the bound charge density on the domain wall can be expressed as a Taylor expansion with respect to η as follows:

$$\sigma_b(x, y) \approx \frac{16 P_0 \alpha x}{r^2 (1 + \alpha)} \eta - \frac{512 P_0 \alpha x (y^2 + \alpha^2 x^2)}{r^6 (1 + \alpha)^3} \eta^3. \quad (\text{A2})$$

If we consider that the maximum deflection of the domain wall is much smaller than the average distance between the pinning centers, i.e., $\eta \ll r$, the electrostatic

potential φ_d can be approximated by the solution of the electrostatic problem where we assume that the bound charges σ_b on the bent domain wall are located at the original position of the domain wall, i.e., at $z = 0$. Then, the electrostatic potential φ_d is given by the solution of the Laplace equation,

$$\varepsilon_c \frac{\partial^2 \varphi_d}{\partial x^2} + \varepsilon_a \left(\frac{\partial^2 \varphi_d}{\partial y^2} + \frac{\partial^2 \varphi_d}{\partial z^2} \right) = 0, \quad (\text{A3a})$$

with the internal boundary conditions for the continuity of the normal component of electric displacement and for the continuity of the electrostatic potential at the domain wall, i.e., at $z = 0$,

$$\frac{\partial \varphi_d^{(+)} }{\partial z} - \frac{\partial \varphi_d^{(-)} }{\partial z} = \frac{\sigma_b}{\varepsilon_0 \varepsilon_a}, \quad \varphi_d^{(+)} = \varphi_d^{(-)}, \quad (\text{A3b})$$

where the superscripts (+) and (−) denote the electrostatic potential for $z > 0$ and $z < 0$, respectively. Considering the periodicity of the bound charge surface density on the domain wall in both the x and y directions with the period equal to r , we will look for a solution of the system of Eq. (A3) in the form of a Fourier series. It can be easily shown that the functions

$$\begin{aligned} \varphi_d^{(\pm)}(x, y, z) = & \sum_{n=1}^{\infty} \phi_{n0} \sin\left(\frac{2n\pi x}{r}\right) e^{\mp(2n\pi z/r) \sqrt{\varepsilon_c/\varepsilon_a}} \\ & + \sum_{n,m=1}^{\infty} \phi_{nm} \sin\left(\frac{2n\pi x}{r}\right) \cos\left(\frac{2m\pi y}{r}\right) \\ & \times e^{\mp(2\pi z/r) \sqrt{m^2+n^2 \varepsilon_c/\varepsilon_a}} \end{aligned} \quad (\text{A4})$$

satisfy the Laplace (A3a). The unknown coefficients ϕ_{n0} and ϕ_{nm} can be found by substituting Eqs. (A2) and (A4) into Eq. (A3b). Straightforward calculations yield the formulae for the unknown coefficients,

$$\begin{aligned} \phi_{n0} = & -\frac{3a\alpha(-1)^n}{n^2\pi^2\varepsilon_0\sqrt{\varepsilon_a\varepsilon_c}(1+\alpha)} \times \\ & \left\{ P_N + \frac{3a^2[18\alpha^2 - n^2\pi^2(1+3\alpha^2)]}{2n^2\pi^2r^2P_0^2(1+\alpha)^2} P_N^3 \right\}, \\ \phi_{nm} = & \frac{54a^3\alpha(-1)^{m+n}}{m^2n\pi^4\varepsilon_0r^2P_0^2\sqrt{m^2\varepsilon_a^2+n^2\varepsilon_c\varepsilon_a}(1+\alpha)^3} P_N^3. \end{aligned} \quad (\text{A5b})$$

After substitution of Eq. (A1) into Eq. (8), the function Φ_{dep} can be expressed in the following forms:

$$\begin{aligned} \Phi_{\text{dep}} = & -\frac{P_0}{ar^2} \int_A u_x(x, y) \varphi_d(x, y, 0) dA \\ = & \sum_{n=1}^{\infty} \frac{-6\alpha(-1)^n P_N}{n\pi r(1+\alpha)} \phi_{n0}. \end{aligned} \quad (\text{A6})$$

It should be noted that the coefficients ϕ_{nm} do not enter the formula for Φ_{dep} because the function $u_x(x, y)$ does not depend on y and the integration of all terms with

$\cos(2m\pi y/r)$ over its period r gives zero. After further substitution of Eq. (A5) into Eq. (A6) and performing the summation, the Taylor expansion of the Φ_{dep} with respect to the net spontaneous polarization is equal to

$$\Phi_{\text{dep}} \approx \frac{0.174a\alpha^2}{\varepsilon_0 r(1+\alpha)^2 \sqrt{\varepsilon_a \varepsilon_c}} \left[P_N^2 - \frac{3a^2(1+1.43\alpha^2)}{2P_0^2 r^2(1+\alpha)^2} P_N^4 \right]. \quad (\text{A7})$$

- ¹U. Robels and G. Arlt, *Journal of Applied Physics* **73**, 3454 (1993), URL <http://link.aip.org/link/?JAP/73/3454/1>.
- ²K. Carl and K. H. Hardtl, *Ferroelectrics* **17**, 473 (1978).
- ³T. J. Yang, V. Gopalan, P. J. Swart, and U. Mohideen, *Phys. Rev. Lett.* **82**, 4106 (1999).
- ⁴D. Schrade, R. Mueller, D. Gross, T. Utschig, V. Y. Shur, and D. C. Lupascu, *Mechanics of Materials* **39**, 161 (2007).
- ⁵W. L. Warren, D. Dimos, B. A. Tuttle, G. E. Pike, R. W. Schwartz, P. J. Clews, and D. C. McIntyre, *Journal of Applied Physics* **77**, 6695 (1995), URL <http://link.aip.org/link/?JAP/77/6695/1>.
- ⁶W. Kleemann, J. Dec, S. A. Prosandeev, T. Braun, and P. A. Thomas, *Ferroelectrics* **334**, 3 (2006).
- ⁷W. Kleemann, *Annual Review of Materials Research* **37**, 415 (2007).
- ⁸T. Braun, W. Kleemann, J. Dec, and P. A. Thomas, *Physical Review Letters* **94**, 117601 (pages 4) (2005), URL <http://link.aps.org/abstract/PRL/v94/e117601>.
- ⁹P. Mokry, *Ferroelectrics* **375**, 40 (2008).
- ¹⁰M. I. Morozov and D. Damjanovic, *Journal of Applied Physics* **104**, 034107 (pages 8) (2008), URL <http://link.aip.org/link/?JAP/104/034107/1>.
- ¹¹S. Li, W. Cao, and L. E. Cross, *Journal of Applied Physics* **69**, 7219 (1991), URL <http://link.aip.org/link/?JAP/69/7219/1>.
- ¹²D. V. Taylor and D. Damjanovic, *Journal of Applied Physics* **82**, 1973 (1997), URL <http://link.aip.org/link/?JAP/82/1973/1>.
- ¹³D. V. Taylor and D. Damjanovic, *Applied Physics Letters* **73**, 2045 (1998), URL <http://link.aip.org/link/?APL/73/2045/1>.
- ¹⁴F. Xu, S. Trolier-McKinstry, W. Ren, B. M. Xu, Z. L. Xie, and K. J. Hemker, *Journal of Applied Physics* **89**, 1336 (2001), URL <http://link.aip.org/link/?JAP/89/1336/1>.
- ¹⁵N. B. Gharb and S. Trolier-McKinstry, *Journal of Applied Physics* **97**, 064106 (pages 7) (2005), URL <http://link.aip.org/link/?JAP/97/064106/1>.
- ¹⁶Y. Zhang and D. C. Lupascu, *Journal of Applied Physics* **100**, 054109 (pages 8) (2006), URL <http://link.aip.org/link/?JAP/100/054109/1>.
- ¹⁷N. Bassiri-Gharb, I. Fujii, E. Hong, S. Trolier-McKinstry, D. V. Taylor, and D. Damjanovic, *Journal of Electroceramics* **19**, 49 (2007).
- ¹⁸A. Kopal, T. Bahník, and J. Fousek, *Ferroelectrics* **202**, 267 (1997).
- ¹⁹A. Kopal, P. Mokry, J. Fousek, and T. Bahník, *Ferroelectrics* **223**, 127 (1999).
- ²⁰A. M. Bratkovsky and A. P. Levanyuk, *Phys. Rev. Lett.* **84**, 3177 (2000).
- ²¹P. Mokry, A. K. Tagantsev, and N. Setter, *Phys. Rev. B* **70**, 172107 (2004).
- ²²N. Odagawa and Y. Cho, *Japanese Journal of Applied Physics* **45**, 7560 (2006).
- ²³K. Fujimoto and Y. Cho, *Japanese Journal of Applied Physics* **43**, 2818 (2004).
- ²⁴A. Amin, M. J. Haun, B. Badger, H. McKinstry, and L. E. Cross, *Ferroelectrics* **65**, 107 (1985).
- ²⁵M. Haun, E. Furman, S. Jang, and L. Cross, *Ferroelectrics* **99**, 63 (1989).
- ²⁶V. Porokhonsky and et.al., (to be published).
- ²⁷J. Hlinka, *Ferroelectrics* **375**, 132 (2008).
- ²⁸B. Meyer and D. Vanderbilt, *Phys. Rev. B* **65**, 104111 (2002).